Title

Distinct Characteristics of Indole-3-Acetic Acid and Phenylacetic Acid, Two Common Auxins in Plants.

Journal

Plant & cell physiology, 56(8)

ISSN

0032-0781

Authors

Sugawara, Satoko
Mashiguchi, Kiyoshi
Tanaka, Keita
et al.

Publication Date

2015-08-01

DOI

10.1093/pcp/pcv088

Peer reviewed

PCP
PLANT & CELL PHYSIOLOGY

Distinct Characteristics of Indole-3-Acetic Acid and Phenylacetic Acid, Two Common Auxins in Plants

Satoko Sugawara[1,11], Kiyoshi Mashiguchi[1,11], Keita Tanaka[1,2,11], Shojiro Hishiyama[3], Tatsuya Sakai[4], Kousuke Hanada[5], Kaori Kinoshita-Tsujimura[6], Hong Yu[7], Xinhua Dai[8], Yumiko Takebayashi[1], Noriko Takeda-Kamiya[1], Tatsuo Kakimoto[6], Hiroshi Kawaide[2], Masahiro Natsume[2], Mark Estelle[7], Yunde Zhao[8], Ken-ichiro Hayashi[9], Yuji Kamiya[1] and Hiroyuki Kasahara[1,10,*]

[1]RIKEN Center for Sustainable Resource Science, Yokohama, Kanagawa, 230-0045 Japan
[2]United Graduate School of Agricultural Science, Tokyo University of Agriculture & Technology, Tokyo, 183-8509 Japan
[3]Forestry and Forest Products Research Institute, Ibaraki, 305-8687 Japan
[4]Graduate School of Science and Technology, Niigata University, Niigata, 950-2181 Japan
[5]Department of Bioscience and Bioinformatics, Kyushu Institute of Technology, Fukuoka, 820-8502 Japan
[6]Department of Biological Sciences, Graduate School of Science, Osaka University, Osaka, 560-0043 Japan
[7]Section of Cell and Developmental Biology and Howard Hughes Medical Institute, University of California at San Diego, La Jolla, CA 92093-0116, USA
[8]Section of Cell and Developmental Biology, University of California at San Diego, La Jolla, CA 92093-0116, USA
[9]Department of Biochemistry, Okayama University of Science, Okayama, 700-0005 Japan
[10]Japan Science and Technology Agency (JST), Precursory Research for Embryonic Science and Technology (PRESTO), Saitama, 332-0012 Japan
[11]These authors contributed equally to this work.
*Corresponding author: E-mail, kasahara@riken.jp; Fax, +81-045-503-9664.
(Received February 9, 2015; Accepted June 7, 2015)

Regular Paper

The phytohormone auxin plays a central role in many aspects of plant growth and development. IAA is the most studied natural auxin that possesses the property of polar transport in plants. Phenylacetic acid (PAA) has also been recognized as a natural auxin for >40 years, but its role in plant growth and development remains unclear. In this study, we show that IAA and PAA have overlapping regulatory roles but distinct transport characteristics as auxins in plants. PAA is widely distributed in vascular and non-vascular plants. Although the biological activities of PAA are lower than those of IAA, the endogenous levels of PAA are much higher than those of IAA in various plant tissues in Arabidopsis. PAA and IAA can regulate the same set of auxin-responsive genes through the TIR1/AFB pathway in Arabidopsis. IAA actively forms concentration gradients in maize coleoptiles in response to gravitropic stimulation, whereas PAA does not, indicating that PAA is not actively transported in a polar manner. The induction of the *YUCCA* (*YUC*) genes increases PAA metabolite levels in Arabidopsis, indicating that YUC flavin-containing monooxygenases may play a role in PAA biosynthesis. Our results provide new insights into the regulation of plant growth and development by different types of auxins.

Keywords: Auxin transport • Indole-3-acetic acid • Metabolism • Phenylacetic acid • Signal transduction.

Abbreviations: Aux/IAA, AUXIN/INDOLE-3-ACETIC ACID; FDR, false discovery rate; gFW, gram fresh weight; GH3, GRETCHEN HAGEN 3; GST, glutathione *S*-transferase; GUS, β-glucuronidase; LC-ESI-MS/MS, liquid chromatography–electrospray ionization–tandem mass spectrometry; MS, Murashige and Skoog; NAA, 1-naphthaleneacetic acid; NPA, 1-*N*-naphthylphthalamic acid; PAA, phenylacetic acid; PAA-Asp, PAA-aspartate; PAA-Glu, PAA-glutamate; TAA1, TRYPTOPHAN AMINOTRANSFERASE OF ARABIDOPSIS 1; TIR1/AFB, TRANSPORT INHIBITOR RESPONSE 1/AUXIN SIGNALING F-BOX; UPLC, ultra performance liquid chromatography; WT, wild-type; YUC, YUCCA.

Introduction

IAA is a signaling molecule that controls plant cell division, cell elongation and differentiation in a concentration-dependent manner (Davies 2004). Plants mainly produce IAA from tryptophan by a two-step reaction that is spatiotemporally regulated (Cheng et al. 2006, Zhao 2012, Brumos et al. 2014). In Arabidopsis, TRYPTOPHAN AMINOTRANSFERASE OF ARABIDOPSIS 1 (TAA1) converts tryptophan to indole-3-pyruvate (IPA), and YUCCA (YUC) flavin-containing monooxygenases catalyze the conversion of IPA to IAA (Stepanova et al. 2008, Tao et al. 2008, Mashiguchi et al. 2011, Stepanova et al. 2011, Won et al. 2011). Previous studies have demonstrated that membrane-localized proteins, including PIN efflux carriers, AUXIN1/LIKE-AUX1 (AUX1/LAX) influx transporters, ABCB transporters and endoplasmic reticulum (ER)-localized carriers, modulate cellular IAA concentrations (Friml 2010, Barbez et al. 2012, Swarup and Peret 2012). PIN efflux carriers are thought to play a crucial role in polar auxin transport to form IAA concentration gradients. Various IAA inactivation enzymes that catalyze oxidation, methylation, and conjugation with amino acids or sugars also regulate the cellular IAA concentration (Korasick et al. 2013). Recent genetic and biochemical studies have indicated that the 2-oxindole-3-acetic

Plant Cell Physiol. 56(8): 1641–1654 (2015) doi:10.1093/pcp/pcv088, Advance Access publication on 14 June 2015, available online at www.pcp.oxfordjournals.org

acid pathway and the GRETCHEN HAGEN 3 (GH3)-dependent amino acid conjugation pathway probably play major roles in the inactivation of IAA (Staswick et al. 2005, Pěnčík et al. 2013, Zhao et al. 2013, Tanaka et al. 2014). In the nucleus, IAA enhances the interaction of TRANSPORT INHIBITOR RESPONSE 1/AUXIN SIGNALING F-BOX (TIR1/AFB) proteins with AUXIN/INDOLE-3-ACETIC ACID (Aux/IAA) transcriptional repressors and promotes the ubiquitination of Aux/IAAs by the SKP1 (S-PHASE KINASE-ASSOCIATED PROTEIN 1)–CULLIN-F-BOX (SCF) E3-ligase complex (Dharmasiri et al. 2005, Kepinski and Leyser 2005, Calderon-Villalobos et al. 2010). Degradation of polyubiquitinated Aux/IAAs by the 26S–proteasome pathway induces the expression of various auxin-responsive genes via auxin response factors (ARFs).

Phenylacetic acid (PAA) is a naturally occurring auxin previously found in vascular plants and seaweeds (Korasick et al. 2013). PAA was initially tested as an artificial auxin by Haagen Smit and Went in 1935 (Haagen Smit and Went 1935). Since then, it has been reported that PAA shows biological activity in classical auxin assays; for example, PAA significantly stimulates the elongation of coleoptile segments of oats (*Avena sativa*) and internodal segments of beans (*Phaseolus vulgaris*) (Haagen Smit and Went 1935, Muir et al. 1967, Small and Morris 1990). The biological activity of PAA is generally lower than that of IAA, but it has been reported that PAA, rather than IAA, actively promotes the formation of lateral roots in peas (*Pisum sativum*) (Schneider et al. 1985). PAA exists at physiologically significant levels in several plant species such as tomatoes, tobacco, sunflowers, peas, barley and maize (Wightman and Lighty 1982, Schneider et al. 1985). A previous study using *Tropaeolum majus* (Nasturtium) suggested that PAA might be produced from the nitrilase-dependent pathway using benzylglucosinolate as a precursor (Ludwig-Müller and Cohen 2002). However, we recently demonstrated that the YUC6 protein expressed in *Escherichia coli* was able to convert phenylpyruvate (PPA) to PAA (Dai et al. 2013), suggesting that PAA might be produced from PPA in plants. Hence, it is still unclear how PAA is synthesized in plants. Active and polar auxin transport profiles of IAA have been demonstrated in various plant tissues; ^{14}C-labeled IAA is directionally transported in the stem segments of light-grown peas (Morris and Johnson 1987), etiolated epicotyl segments of peas (Procházka and Borkovec 1984) and petiole segments of cotton (Suttle and Mansager 1986). On the other hand, the movement of ^{14}C-labeled PAA is limited and exhibits little, if any, polarity in the same plant tissues (Procházka and Borkovec 1984, Suttle and Mansager 1986, Morris and Johnson 1987). Interestingly, a previous study reported that PAA inhibits the polar transport of ^{14}C-labeled IAA in intact plants and stem segments of peas (Morris and Johnson 1987). Morris and Johnson proposed that PAA could play an indirect role in growth regulation by modulating the polar transport and/or accumulation by cells of IAA (Morris and Johnson 1987). It is important to investigate further PAA transport using other in vivo systems to understand the role of PAA in plants. It has been reported that PAA binds to AUXIN BINDING PROTEIN 1 (ABP1) from maize (Löbler and Klämbt 1985), but the direct interaction of PAA with TIR1/AFB and Aux/IAA proteins has yet to be investigated (Shimizu-Mitao and Kakimoto 2014). Although the molecular basis of the biosynthesis, inactivation, transport and signal transduction of PAA remains largely unknown (Simon and Petrasek 2011, Korasick et al. 2013), previous studies suggest that IAA and PAA may play different roles as auxins in plants.

In this study, we demonstrate that PAA is widely distributed in vascular and non-vascular plants. The analysis of perception mechanisms and auxin-inducible genes indicates that IAA and PAA probably have overlapping regulatory roles as auxins. We further demonstrate that endogenous IAA and PAA show different transport characteristics in maize coleoptiles. The YUC family may be implicated in both IAA and PAA biosynthesis in Arabidopsis. We provide new insights into the regulation of plant growth and development by different types of auxins.

Results

PAA is widely distributed in vascular and non-vascular plants

To investigate the distribution of PAA in the plant kingdom, we first measured the endogenous levels of IAA and PAA in Arabidopsis, oats, barley, the moss *Physcomitrella patens* and the liverwort *Marchantia polymorpha* using liquid chromatography–electrospray ionization–tandem mass spectrometry (LC-ESI-MS/MS). Similar to IAA, PAA was detected at significant levels in Arabidopsis seedlings (IAA, 49 ± 2 pmol/gFW; PAA, 413 ± 15 pmol/gFW), young shoots of oats (IAA, 31 ± 2 pmol/gFW; PAA, 3,860 ± 220 pmol/gFW), young shoots of barley (IAA, 30 ± 2 pmol/gFW; PAA, 4,353 ± 353 pmol/gFW), *P. patens* (IAA, 14 ± 4 pmol/gFW; PAA, 1,049 ± 278 pmol/gFW) and *M. polymorpha* (IAA, 74 ± 10 pmol/gFW; PAA, 469 ± 103 pmol/gFW). PAA was widely distributed in both vascular and non-vascular plants, and the endogenous concentrations of PAA were higher than those of IAA in all plant species we analyzed.

We next investigated the endogenous concentrations of IAA and PAA in various tissues in Arabidopsis (**Fig. 1**). The levels of IAA varied depending on the plant tissue and were remarkably higher in dry seeds and siliques than in other tissues. Intriguingly, the levels of PAA were 1.7-fold higher than those of IAA in dry seeds, 14.8-fold higher in inflorescences, 13.2-fold higher in cauline leaves, 4-fold higher in stems, 7.6-fold higher in rosette leaves and 8.3-fold higher in roots, while the levels of PAA were 2.4-fold lower than those of IAA in siliques. These results suggest that, similar to IAA (Ljung et al. 2001), the endogenous concentration of PAA may be spatiotemporally regulated in plants.

PAA shows biological activity via the TIR1/AFB-mediated pathway

To address the action mechanism of PAA, we performed several auxin activity tests using Arabidopsis. The application of PAA enhanced the formation of lateral roots, although the activity

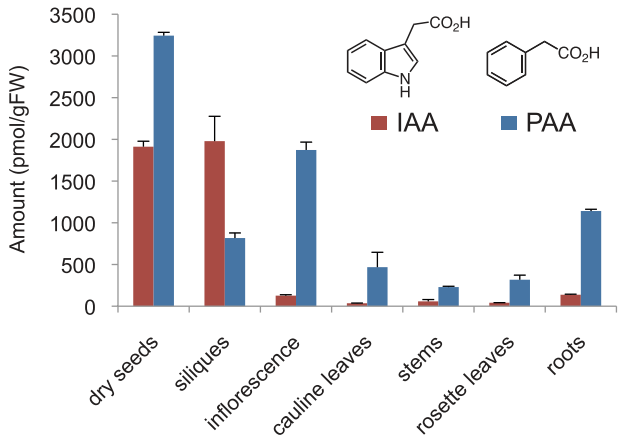

Fig. 1 The endogenous amounts of IAA and PAA in various tissues of Arabidopsis. Dry seeds and tissues from 5–12 plants were pooled for each sample, and three samples were analyzed for each data point. Data are the mean ± SD.

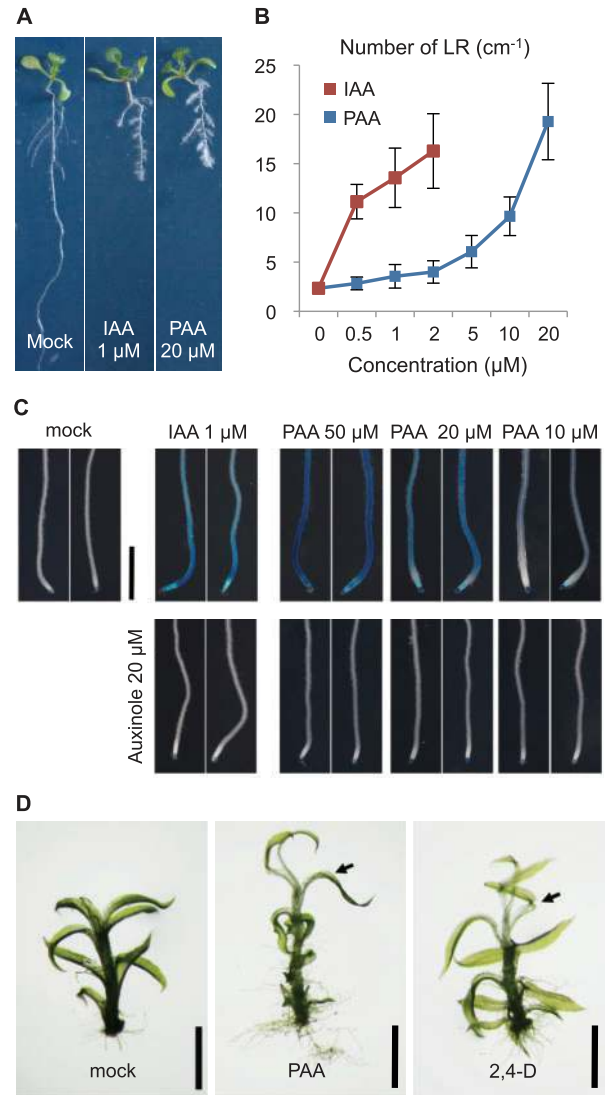

Fig. 2 Auxin activity of PAA on Arabidopsis and *P. patens*. (A and B) Enhancement of lateral root formation on Arabidopsis by IAA and PAA. Data are the mean ± SD (n = 10). (C) GUS expression patterns in *DR5::GUS* plants after IAA or PAA treatment in the absence or presence of auxinole (20 μM). Scale bar = 1 mm. (D) Elongation of gametophores in *P. patens* by PAA (5 μM) and 2,4-D (5 μM). Arrows indicate the auxin-responsive elongation zone. Scale bar = 1 mm.

was 10- to 20-fold lower than that of IAA (**Fig. 2A, B**). PAA induced the DR5-driven expression of β-glucuronidase (GUS) in the roots of *DR5::GUS* plants, although the activity was nearly 20-fold lower than that of IAA (**Fig. 2C**). This PAA-induced GUS expression was abolished by the co-application of auxinole, a specific inhibitor of TIR1/AFBs (**Fig. 2C**) (Hayashi et al. 2012). In addition, we tested the response to PAA in *tir1-1* and *tir1-1 afb2-3* seedlings using the root elongation assay, and demonstrated that the roots of *tir1-1 afb2-3* were resistant to PAA, similarly to IAA (**Supplementary Fig. S1**). These results indicate the involvement of TIR1/AFBs in the PAA signal transduction pathway. In addition, treatment of the moss *P. patens* with PAA, similarly to 2,4-D, led to typical auxin responses such as the elongation of gametophores (**Fig. 2D**) (Hayashi et al. 2008), suggesting that the biological functions of PAA as an auxin are probably evolutionarily conserved in land plants.

To confirm whether PAA functions through the TIR1/AFB-mediated pathway, we analyzed the interaction of PAA and auxin co-receptors using a yeast two-hybrid system (Calderon Villalobos et al. 2012). Among six TIR1/AFBs in Arabidopsis, we used TIR1, AFB2 and AFB5 for the interaction analysis in this study (Parry et al. 2009). As for Aux/IAAs, eight proteins representing distinct subclades were chosen from 29 Aux/IAAs in Arabidopsis (Calderon Villalobos et al. 2012). As shown in **Fig. 3A**, the interaction of TIR1/AFB2/AFB5 with various Aux/IAAs was promoted in the yeast two-hybrid assay with 100 μM IAA as previously reported (Calderon Villalobos et al. 2012). PAA promoted the interaction of relatively limited numbers of TIR1/AFB2/AFB5 and Aux/IAAs in the same concentration used for IAA (100 μM). When the interaction test was carried out with 1 mM PAA, TIR1/AFB2/AFB5–Aux/IAA interaction profiles were similar to those observed in 100 μM IAA (**Fig. 3A**). Although the efficiency of auxin uptake into yeast cells may differ between IAA and PAA, these results indicate that PAA can bind to TIR1/AFBs and Aux/IAAs, and that these auxins may have overlapping roles in plants.

To provide direct evidence that PAA binds to auxin co-receptors in vitro, we performed a pull-down assay using TIR1 and IAA3 or IAA7 (Yu et al. 2013). As shown in **Fig. 3B**, 50 μM IAA enhanced the formation of both TIR1–IAA3 and TIR1–IAA7 complexes (3.48- and 5.02-fold, respectively) compared with those in the control. We found that PAA also enhanced the formation of a TIR1–IAA7 complex at the same concentration, while PAA did not significantly enhance the formation of a TIR1–IAA3 complex (**Fig. 3B**), suggesting that these auxins have different affinities for various auxin co-receptors. Taken together, these results indicate that PAA functions through the TIR1/AFB-mediated pathway and that IAA and PAA probably have overlapping roles, but may generate different output from auxin perception.

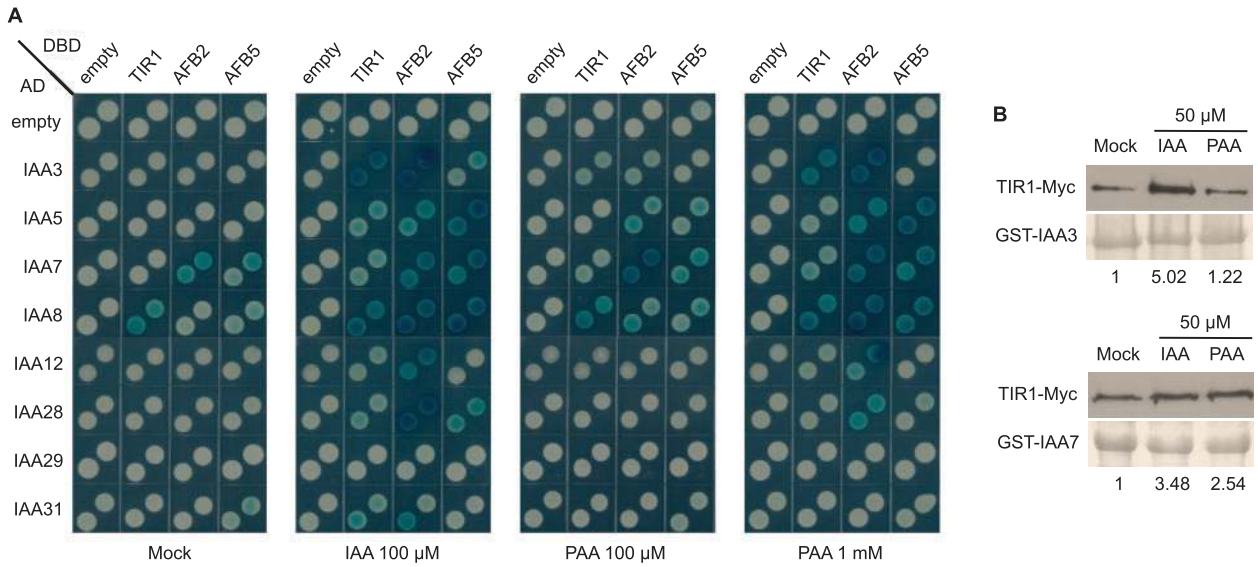

Fig. 3 Promotion of TIR1/AFB–Aux/IAA interaction by auxins. (A) Yeast two-hybrid assay showing that PAA promotes the interaction between TIR1/AFB2/AFB5 and Aux/IAAs. (B) In vitro pull-down assay showing that both IAA and PAA enhance the interaction between TIR1-Myc and GST–IAA7, while PAA does not strongly enhance the interaction of TIR1-Myc with GST–IAA3. Numbers indicate the relative differences from the control sample.

IAA and PAA regulate the same auxin-responsive genes

To investigate the genes regulated by PAA, we performed microarray analyses using Arabidopsis seedlings treated with IAA or PAA. We analyzed the genes regulated by IAA (1 μM) or PAA (10 μM) within 1 h to confirm whether PAA can induce early auxin-responsive genes such as *GH3* and *Aux/IAA* genes. We identified a total of 169 genes regulated by IAA (136 genes) and/or PAA (53 genes) in our data set [false discovery rate (FDR) < 0.05, **Supplementary Table S1**]. The correlated analysis of 169 genes using fold change values showed that almost all genes were regulated by both IAA and PAA in the same manner (**Fig. 4**). As shown in **Table 1** (FDR < 0.05), the top 15 genes up-regulated by both PAA and IAA include *GH3* genes (*GH3.2*, *GH3.3*, *GH3.4* and *GH3.5*), *Aux/IAA* genes (*IAA1*, *IAA2*, *IAA5* and *IAA13*) and known auxin-up-regulated genes such as *ASYMMETRIC LEAVES2-LIKE 16/LATERAL ORGAN BOUNDARIES-DOMAIN 29* (*ASL16/LBD29*) and *HAT2*, which have also been identified as IAA-up-regulated genes in previous reports (Goda et al. 2004, Nemhauser et al. 2006). Based on FDR (<0.05) and fold changes (>2), no genes specifically regulated by IAA or PAA were identified in our data set. These results indicate that IAA and PAA have overlapping regulatory roles as auxins in Arabidopsis.

IAA and PAA show distinct distribution patterns in maize coleoptiles on auxin transport inhibitor treatment and gravitropic stimulation

We next studied PAA movement by analyzing the distribution patterns of endogenous auxins in maize coleoptiles. As previously reported, we prepared four segments from etiolated maize coleoptiles by horizontal sectioning and measured auxin levels in each segment (**Fig. 5A–C**) (Nishimura et al. 2009). IAA formed concentration gradients from the tip downward in coleoptiles (mock), with the highest level in the tip region, where IAA is most actively produced (**Fig. 5B**) (Nishimura et al. 2009). In agreement with this, *VT2* and *SPI1* genes, which encode co-orthologs of *TAA1* and *YUC* genes, were expressed at a higher level in the tip region (**Fig. 5D**) (Gallavotti et al. 2008, Phillips et al. 2011). As shown in **Fig. 5C**, we found that PAA formed a similar gradient pattern with IAA in coleoptiles (mock), suggesting that both IAA and PAA may be actively produced in the tip region in maize coleoptiles. To investigate the mechanism of PAA movement, we applied the polar auxin transport inhibitor 1-*N*-naphthylphthalamic acid (NPA) to the tip region of maize coleoptiles

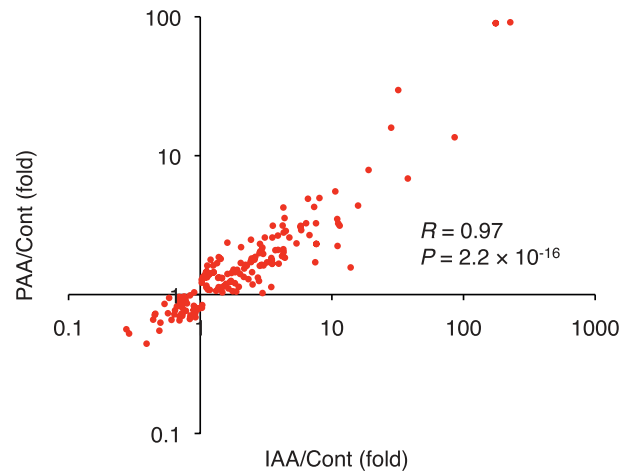

Fig. 4 Correlation analysis of early IAA- and PAA-regulated genes in Arabidopsis. Each dot represents a gene regulated by IAA and/or PAA (FDR < 0.05). *x*- and *y*-axes indicate fold changes in expression intensities for IAA and PAA compared with mock treatment, respectively.

Table 1 IAA- and PAA-up-regulated genes in Arabidopsis

AGI code	Name	IAA up-regulated (IAA/control)	PAA up-regulated (PAA/contriol)
AT2G23170	*GH3.3*	226.5	91.3
AT1G59500	*GH3.4*	175.7	90.0
AT4G37390	*GH3.2*	175.7	90.0
AT3G58190	*ASL16/LBD29*	31.9	29.7
AT2G39370	–	28.2	15.9
AT1G15580	*IAA5*	85.6	13.6
AT5G47370	*HAT2*	19.0	7.9
AT4G27260	*GH3.5*	10.6	5.5
AT3G23030	*IAA2*	8.0	5.0
AT1G78100	–	6.6	4.9
AT4G13195	*CLE44*	4.3	4.2
AT5G52900	–	4.4	3.6
AT4G14560	*IAA1*	11.2	3.3
AT5G41400	–	4.2	3.1
AT2G33310	*IAA13*	3.9	2.7

The top 15 genes with a ratio (IAA/control or PAA/control) of >2 and FDR < 0.05 are listed.

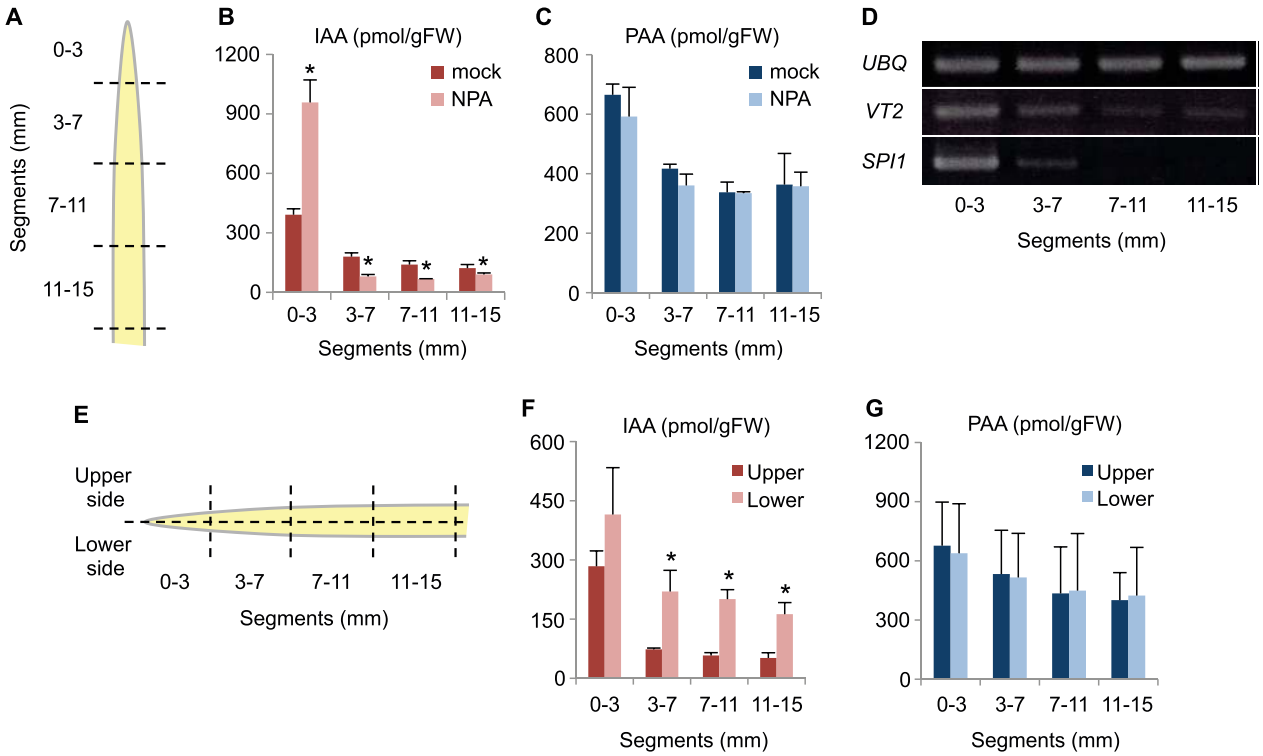

Fig. 5 Distribution patterns of IAA and PAA in maize coleoptiles. (A) Schematic representation of maize coleoptile segments. NPA was applied to the tip region (0–3 mm). (B and C) Distinct distribution patterns of IAA (B) and PAA (C) in maize coleoptile segments treated with mock solution (mock) or 200 μM NPA for 1 h (NPA). Asterisks indicate significant differences from the mock segment (Student's *t*-test, $P < 0.05$). (D) Expression patterns of *VT2* and *SPI1* genes in maize coleoptiles. *UBQ*, ubiquitin as control. (E) Schematic representation of maize coleoptile segments under gravitropic stimulation. (F and G) Distinct distribution pattern of IAA (F) and PAA (G) in maize coleoptile segments after gravitropic stimulation. Segments from 5–10 coleoptiles were pooled for each sample, and three samples were analyzed for each data point. Data are the mean ± SD. Asterisks indicate a significant difference from the upper segment (Student's *t*-test, $P < 0.05$).

(Nishimura et al. 2009) and measured the level of auxins (Fig. 5B, C). NPA blocked the basipetal transport of IAA and elevated IAA levels by 2.4-fold in the tip region (0–3 mm), and decreased those in the lower regions (from 3–7 mm to 11–15 mm) (Fig. 5B). In contrast, NPA treatment did not affect PAA gradient patterns (Fig. 5C), suggesting that PAA is not actively transported basipetally in maize coleoptiles. However, we cannot exclude the possible involvement of unknown NPA-insensitive transport machinery.

Furthermore, we investigated auxin gradient patterns in maize coleoptiles under gravitropic stimulation. As shown in Fig. 5E, etiolated coleoptiles were maintained in a horizontal position for 1 h in the dark and used to prepare eight segments by vertical and horizontal sectioning. We observed IAA concentration gradients from the lower to the upper side, with higher concentrations localized at the lower side as reported previously (Fig. 5F) (Nishimura et al. 2009). In contrast, no significant difference in PAA concentration gradients was observed under the same conditions (Fig. 5G), indicating that the movement of PAA is not directional and is comparatively slow in maize coleoptiles. From these results and previous biochemical studies, we concluded that PAA is a common auxin that is not transported actively and directionally in plants.

PAA cannot recover the root gravitropism of *yucQ* mutants

To demonstrate further the distinct characteristics of IAA and PAA, we next investigated the recovery of root phenotypes of *yuc3 yuc5 yuc7 yuc8 yuc9* quintuple (*yucQ*) mutants with IAA and PAA (Won et al. 2011, Chen et al. 2014). Application of IAA and PAA restored the severe root growth defects of *yucQ* to wild-type (WT) levels (Fig. 6A, B). No significant increase in IAA levels was observed in roots of *yucQ* by treatment with PAA (Fig. 6C). Similarly, PAA levels were not significantly increased in roots of *yucQ* by treatment with IAA (Fig. 6D). When these seedlings were grown horizontally for 24 h, the IAA-restored primary roots of *yucQ* showed a positive response to gravitropic stimulation (Fig. 6E). In contrast, no significant response was observed in the PAA-restored primary roots of *yucQ* (Fig. 6E). These results suggest that IAA generates concentration gradients, but PAA does not, in response to gravitropic stimulation; thus, these natural auxins have distinct transport characteristics.

In addition to IAA and PAA, we examined the recovery of root phenotypes of *yucQ* with the synthetic auxins 1-naphthaleneacetic acid (NAA) and 2,4-D. NAA and 2,4-D are well-characterized synthetic auxins that show IAA-like biological activities, and the latter has been used commercially as a potent herbicide for >50 years (Van Overbeek 1959). Similar to IAA, NAA is actively and directionally transported in various plant tissues and in suspension-cultured plant cells (Fig. 6F), whereas the movement of 2,4-D is limited in plant tissues and in suspension-cultured plant cells (Beyer 1972, Delbarre et al. 1996, Jacobs et al. 1966). The AUX1/LAX family can transport IAA and 2,4-D, but probably does not contribute to the uptake of NAA by cells (Yamamoto and Yamamoto 1998, Yang et al. 2006, Friml 2010) (Fig. 6F). NAA and 2,4-D restored the severe root growth defects of *yucQ* to WT levels without a significant increase of IAA or PAA levels (Fig. 6A–D). When NAA- or 2,4-D-restored *yucQ* seedlings were grown horizontally for 24 h, the NAA-restored primary roots showed a positive response to gravitropic stimulation, but no significant response was observed in the 2,4-D-restored primary roots (Fig. 6E). These results indicate that the transport characteristics of 2,4-D are similar to those of PAA, but are different from those of IAA and NAA (Fig. 6F).

A possible role for the TAA and YUC families in PAA biosynthesis

Because IAA and PAA exist widely in vascular and non-vascular plants, we hypothesized that IAA biosynthetic enzymes are also implicated in PAA synthesis. The YUC family catalyzes a rate-limiting step of the IPA pathway in IAA biosynthesis (Fig. 7A) (Mashiguchi et al. 2011). Overexpression of *YUC* genes promotes IAA production and results in high-auxin phenotypes, such as hypocotyl elongation, primary root growth inhibition and enhanced lateral root growth (Mashiguchi et al. 2011, Zhao et al. 2001). To test our hypothesis in vivo, we investigated the metabolic impact of *YUC* overexpression on PAA biosynthesis using Arabidopsis with β-estradiol-inducible *YUC1* (*YUC1ox*), *YUC2* (*YUC2ox*) or *YUC6* (*YUC6ox*) (Fig. 7B). Treatment with β-estradiol increased *YUC1*, *YUC2* and *YUC6* expression levels by 41-, 142- and 29-fold in *YUC1ox*, *YUC2ox* and *YUC6ox* plants, respectively, compared with those in the vector control plants (*pER8*) (Supplementary Fig. S2). As shown in Fig. 7C, the induction of *YUC* genes greatly increased the levels of the IAA metabolites IAA-aspartate (IAA-Asp) and IAA-glutamate (IAA-Glu) compared with those in *pER8* plants, probably due to a rapid inactivation of increased IAA by the GH3 family (Mashiguchi et al. 2011). We assumed that the levels of the possible PAA metabolites PAA-aspartate (PAA-Asp) and PAA-glutamate (PAA-Glu) would be increased by the induction of *YUC* genes if the YUC family were involved in PAA biosynthesis (Fig. 7A). To this end, we synthesized ^{13}C-labeled PAA-Asp and PAA-Glu as internal standards and established analysis methods for measuring the levels of these potential PAA metabolites using LC-ESI-MS/MS. The induction of *YUC* genes remarkably elevated PAA-Asp and PAA-Glu levels by 14- to 41-fold and 1.6- to 3.8-fold, respectively, in *YUC1ox*, *YUC2ox* and *YUC6ox* plants compared with those in *pER8* plants (Fig. 7D). These results indicate that the YUC family may be involved in PAA biosynthesis in Arabidopsis (Fig. 7A).

In addition, we examined the enzymatic conversion of PPA to PAA by glutathione *S*-transferase (GST)-fused YUC2 proteins expressed in *E. coli*. As shown in Fig. 7E, GST-fused YUC2 proteins converted IPA to IAA, and the reaction was abolished in the absence of NADPH. Similarly, we detected the conversion of PPA to PAA with GST–YUC2 proteins by the decrease of a specific ion for PPA at 3.6 min and the increase of a specific ion for PAA at 4.8 min using LC-ESI-MS/MS (Fig. 7F). The conversion of PPA to PAA with GST–YUC2 was abolished in

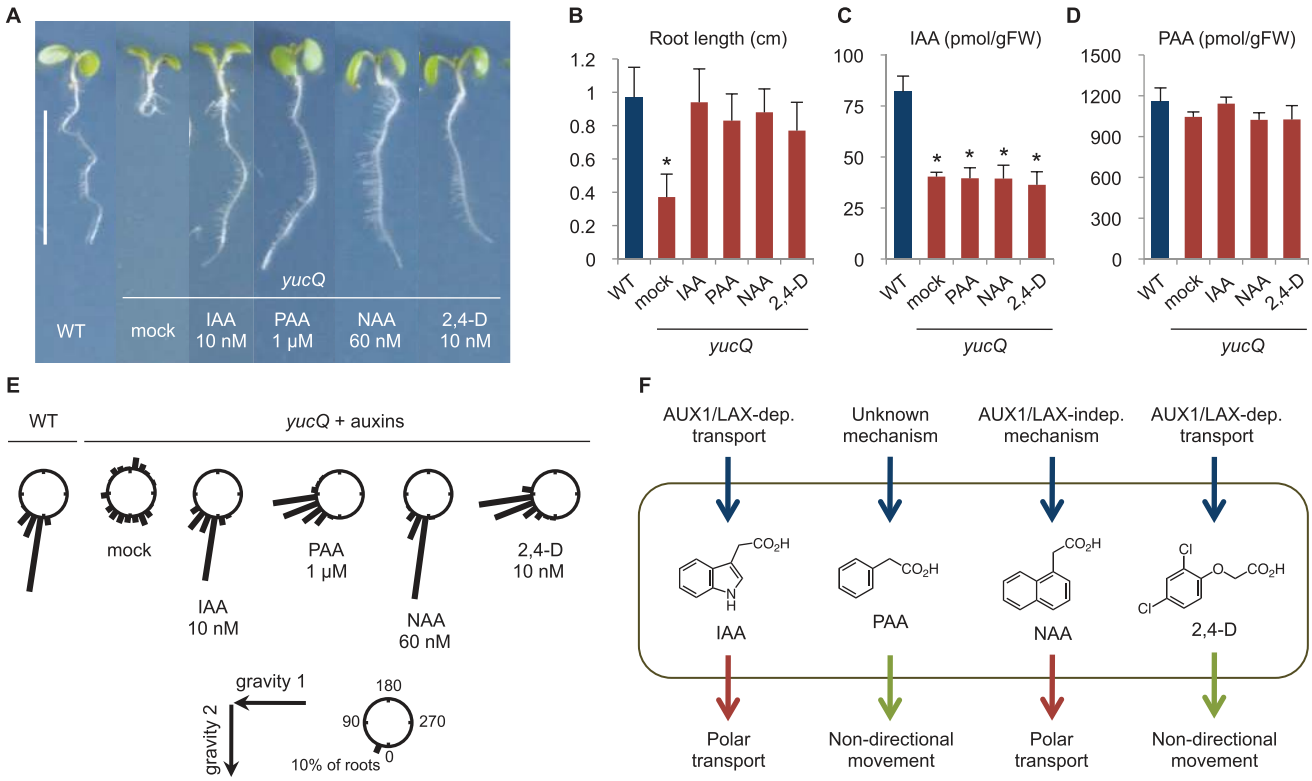

Fig. 6 Recovery of the root growth in *yucQ* by IAA and PAA. (A and B) Recovery of primary root length in *yucQ* by auxins. Scale bar = 1 cm. Data are the mean ± SD ($n = 60$). The asterisk indicates a significant difference from the WT (Student's *t*-test, $P < 0.05$). (C and D) Endogenous levels of IAA and PAA in roots of auxin-treated *yucQ*. Roots from 60–70 seedlings were pooled for each sample, and three samples were analyzed for each data point. Data are the mean ± SD. Asterisks indicate a significant difference from the WT (Student's *t*-test, $P < 0.05$). (E) Effect of auxins on the gravitropic response of *yucQ*. The frequencies (%) of root growth direction at intervals of 15° are represented by the lengths of the bars ($n = 50$). (F) Schematic representation of transport profiles of auxins in a plant cell.

the absence of NADPH, similar to the conversion of IPA to IAA (**Fig. 7E, F**). From these results, we confirmed that YUC proteins catalyze the conversion of PPA to PAA.

To investigate further the involvement of the YUC family in PAA biosynthesis in vivo, we analyzed the endogenous levels of IAA and PAA in *yuc1 yuc2 yuc6* triple knockout mutants. For analysis, we used the inflorescence parts of *yuc1 yuc2 yuc6* because the auxin-deficient phenotypes are obvious in these tissues (**Fig. 7G**). The endogenous levels of IAA were 52% reduced in the inflorescence parts of *yuc1 yuc2 yuc6* compared with those of WT plants (**Fig. 7H**). In contrast, the endogenous amounts of PAA in the same tissues were comparable between *yuc1 yuc2 yuc6* and WT plants (**Fig. 7H**). Similarly, as already shown in **Fig. 6C**, the levels of IAA were 51% reduced, but PAA levels in the roots of *yucQ* were not significantly lower than those in WT plants (**Fig. 6D**). Given that the induction of *YUC* genes can increase PAA synthesis (**Fig. 7D**) and that 11 *YUC* genes occur in Arabidopsis, these results suggest that other active YUC enzymes may contribute to the homeostatic regulation of PAA levels in *yuc1 yuc2 yuc6* or *yucQ* mutants.

To study whether the TAA family is involved in PAA biosynthesis, we analyzed IAA and PAA levels in *TAA1*-deficient *wei8-1* mutants (Stepanova et al. 2008). We used the seeds of *wei8-1* mutants because the seeds of WT plants contain the highest levels of PAA (**Fig. 1**). The levels of IAA were 80% reduced in the seeds of *wei8-1* compared with those in WT plants (**Fig. 7I**). We found that the levels of PAA were 20% lower in the seeds of *wei8-1* than in WT plants (**Fig. 7I**). Taken together with in vitro evidence that TAA1 proteins can convert phenylalanine to PPA (Tao et al. 2008), these results suggest that the TAA family may play a role in PAA biosynthesis in Arabidopsis. However, the levels of PAA were not remarkably decreased compared with those of IAA in *wei8-1* mutants. As four genes closely related to *TAA1* (*TAR1–TAR4*) genes also occur in Arabidopsis (Stepanova et al. 2008), TAR enzymes may participate in the homeostatic regulation of PAA levels in *wei8-1* mutants. In addition, we do not exclude the possibility that other unknown pathways also contribute to PAA biosynthesis in Arabidopsis.

The GH3 family probably plays a role in PAA metabolism

The constitutive occurrence of PAA-Asp and PAA-Glu in vector control plants (*pER8*, **Fig. 7D**) and a pronounced increase in these PAA–amino acid conjugate levels, as well as IAA-Asp and IAA-Glu levels in β-estradiol-induced *YUCox* plants (**Fig. 7C, D**), suggest that the PAA metabolic pathway involves *GH3* genes, which encode enzymes catalyzing the synthesis of

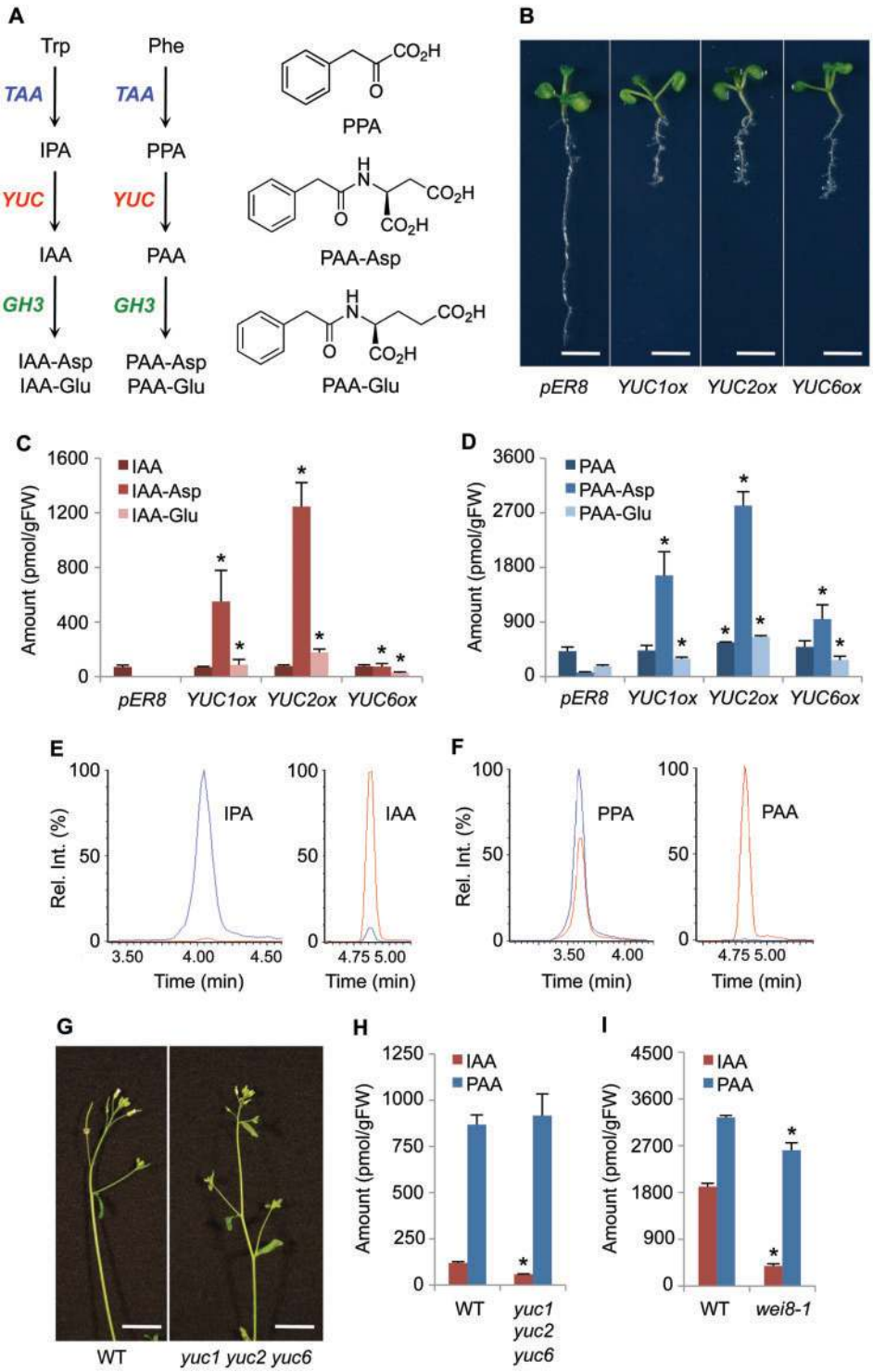

Fig. 7 PAA biosynthesis and inactivation pathways in Arabidopsis. (A) Scheme of biosynthesis and inactivation pathways for IAA and PAA in Arabidopsis. (B) High-auxin phenotypes of *YUCox* plants treated with β-estradiol. Scale bars = 0.5 cm. (C and D) The levels of IAA metabolites (C) and PAA metabolites (D) increase in *YUCox* plants treated with β-estradiol. Whole seedlings were pooled for each sample, and three samples were analyzed for each data point. Data are the mean ± SD. Asterisks indicate a significant difference from *pER8* (Student's *t*-test, $P < 0.05$). (E) Conversion of IPA to IAA by GST–YUC2 proteins. The conversion of IPA to IAA was monitored using a precursor ion (*m*/*z* 202) for IPA at 4.1 min and a product ion (*m*/*z* 130.1) for IAA at 4.8 min in the presence (red) and absence (blue) of NADPH. (F) Conversion of PPA to PAA by GST–YUC2 proteins. The conversion of PPA to PAA was monitored using a product ion (*m*/*z* 91.1) for PPA at 3.6 min and for PAA at 4.8 min in the presence (red) and absence (blue) of NADPH. (G) Phenotypes of WT and *yuc1 yuc2 yuc6* mutants. Scale bar = 1 mm. (H) The endogenous levels of IAA and PAA in the inflorescence parts of the WT and *yuc1 yuc2 yuc6*. Inflorescence parts were pooled for each sample, and three samples were analyzed for each data point. Data are the mean ± SD. Asterisks indicate a significant difference from the WT (Student's *t*-test, $P < 0.05$). (I) The endogenous levels of IAA and PAA in dry seeds of WT and *wei8-1* mutants. Dry seeds were pooled for each sample, and three samples were analyzed for each data point. Data are the mean ± SD. Asterisks indicate a significant difference from the WT (Student's *t*-test, $P < 0.05$).

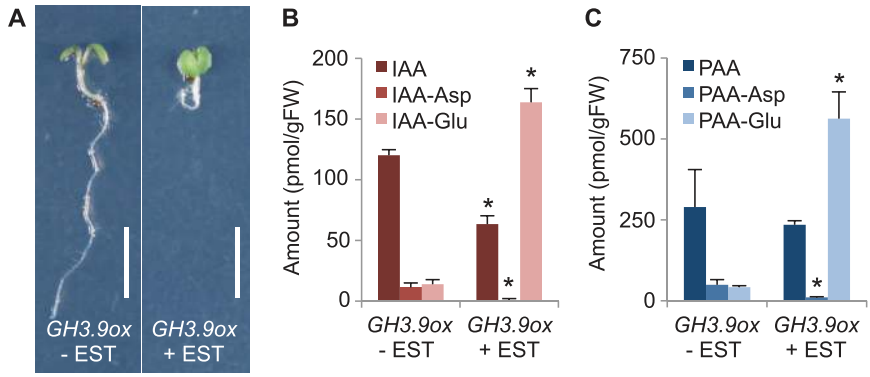

Fig. 8 Metabolism of PAA in *GH3.9ox* plants. (A) Phenotype of *GH3.9ox* plants with or without β-estradiol treatment. Scale bars = 5 mm. Seedlings were treated with 10 μM β-estradiol for 5 d. (B and C) The levels of IAA metabolites (B) and PAA metabolites (C) increase in *GH3.9ox* plants with β-estradiol treatment (+EST). Whole seedlings were pooled for each sample, and three samples were analyzed for each data point. Data are the mean ± SD. Asterisks indicate a significant difference from *GH3.9ox* −EST (Student's *t*-test, $P < 0.05$).

IAA–amino acid conjugates (**Fig. 7A**) (Staswick et al. 2005). To investigate this, we generated transgenic plants expressing β-estradiol-inducible *GH3.9* (*GH3.9ox*). As previously demonstrated in β-estradiol-inducible *GH3.6* (Tanaka et al. 2014), the induction of *GH3.9* resulted in root growth defects and loss of gravitropism (**Fig. 8A**). The induction of *GH3.9* increased the endogenous levels of IAA-Glu by 11-fold (**Fig. 8B**). Similarly, PAA-Glu showed a 13-fold increase in *GH3.9ox* plants (**Fig. 8C**). These results indicate the involvement of the *GH3* family in PAA metabolism in Arabidopsis.

Discussion

Occurrence, biosynthesis and inactivation of PAA in plants

Here, we demonstrated that PAA is a natural auxin widely distributed in both vascular and non-vascular plants, including the moss *P. patens* and the liverwort *M. polymorpha*. For the biosynthesis of PAA, previous studies have demonstrated that TAA1 can convert phenylalanine to PPA and that YUC6 catalyzes the conversion of PPA to PAA in vitro (Tao et al. 2008, Dai et al. 2013). We demonstrated that IAA and PAA levels decreased in *wei8-1* mutants (**Fig. 7I**). Moreover, we demonstrated that the induction of *YUC* genes remarkably increases both IAA and PAA metabolite levels (**Fig. 7C, D**) and the YUC2 protein catalyzes the conversion of PPA to PAA similar to that of IPA to IAA in vitro (**Fig. 7E, F**). Taking these observations together, the TAA and YUC families may be involved in PAA biosynthesis in Arabidopsis (**Fig. 7A**). Intriguingly, we found that the endogenous levels of PAA were not significantly decreased in *yuc1 yuc2 yuc6* and *yucQ*, while IAA reduction is remarkable in those mutants (**Figs. 6C, D**, **7H**). Similarly, the levels of PAA reduction were markedly less than those of IAA reduction in the seeds of *wei8-1* mutants (**Fig. 7I**). The exact mechanisms are still unknown, but it is possible that other YUC or TAR enzymes contribute to maintaining endogenous PAA levels in *yuc* multiple knockout mutants and *wei8-1* mutants. Alternatively, unknown PAA biosynthesis pathways may occur in Arabidopsis. A previous study using *T. majus* suggested that PAA might be produced from the nitrilase-dependent pathway (Ludwig-Müller and Cohen 2002). In Arabidopsis, it has been reported that IAA is generated partially from tryptophan through indole-3-acetaldoxime (IAOx), a key intermediate of indole-glucosinolates (Sugawara et al. 2009). Cyt P450 monooxygenases encoded by the *CYP79B* family catalyze the conversion of tryptophan to IAOx (Hull et al. 2000, Mikkelsen et al. 2000). The occurrence of the *CYP79B* family is limited to glucosinolate-producing plants (Bak et al. 1998), suggesting an auxiliary role for the IAOx pathway in IAA biosynthesis in plants. Similarly, CYP79A2 mediates the conversion of phenylalanine to phenylacetaldoxime (PAOx) in phenyl-glucosinolate biosynthesis in Arabidopsis (Wittstock and Halkier 2000). As the chemical structures of IAOx and PAOx are similar, PAA might be produced partially from PAOx. Further investigation is required to understand PAA biosynthesis and its regulation in plants.

The GH3 family plays an important role in IAA homeostasis (Korasick et al. 2013). Staswick et al. (2005) previously demonstrated that GH3 proteins are able to convert various natural and synthetic auxins, including IAA, PAA and NAA, to their corresponding amino acid conjugates in vitro. Consistent with this, the induction of the *GH3.9* gene significantly increased PAA-Glu levels in Arabidopsis (**Fig. 8C**), indicating the likely role of the GH3 family in PAA metabolism. Intriguingly, the induction of *YUC* genes resulted in high-auxin phenotypes but only slightly increased IAA and PAA levels (**Fig. 7B–D**). Given that IAA– and PAA–amino acid conjugate levels are remarkably increased in *YUCox* plants (**Fig. 7C, D**), we assume that the induction of *YUC* genes promotes the biosynthesis of IAA and PAA, but the GH3 family actively metabolizes these two auxins. In addition to GH3, a glycosyltransferase encoded by the *UGT84B1* gene and a methyltransferase encoded by the *IAMT1* gene have been identified as other IAA metabolic enzymes in Arabidopsis (Jackson et al. 2002, Qin et al. 2005). These results indicate that endogenous levels of PAA might also be regulated by glycosylation and methylation.

Previous studies have reported that PAA exists at much higher levels than IAA in tomatoes, tobacco, sunflowers, peas,

barley and maize (Wightman and Lighty 1982), but the endogenous levels of PAA were much lower than those of IAA in *T. majus* (Ludwig-Müller and Cohen 2002). We analyzed PAA in several vascular and non-vascular plants, and demonstrated that the levels of PAA were higher than those of IAA in all of the species examined. However, we found that the levels of IAA and PAA vary among plant tissues; PAA levels are higher in seeds and inflorescences than in stems and rosette leaves in Arabidopsis (**Fig. 1**). In addition, the ratio of IAA to PAA also differs among tissues, and the levels of IAA are higher than those of PAA in siliques (**Fig. 1**). Although a physiological role for PAA remains unknown, these results suggest that plants may strictly regulate PAA levels using biosynthesis and inactivation enzymes depending on developmental and environmental cues.

Transport of PAA in plants

Polar transport has been recognized as one of the fundamental characteristics of auxins, since IAA was first identified as a naturally occurring auxin that moves directionally, generates concentration gradients and promotes cell elongation in plant tissues. However, previous studies using exogenously applied PAA or ^{14}C-labeled PAA have suggested that PAA is another naturally occurring auxin but is not transported in a polar manner (Haagen Smit and Went 1935, Morris and Johnson 1987, Procházka and Borkovec 1984, Suttle and Mansager 1986). Here, we provide further evidence that endogenous IAA and PAA show distinct transport characteristics in maize coleoptiles. We demonstrated that NPA, an auxin transport inhibitor, effectively inhibits basipetal IAA transport, but not PAA transport, in maize coleoptiles (**Fig. 5B, C**), which is consistent with a previous study using ^{14}C-labeled auxins and cotton petiole segments (Suttle and Mansager 1986). Moreover, unlike IAA, PAA does not form concentration gradients by active and directional transport in response to gravitropic stimulation (**Fig. 5F, G**). Because of the occurrence of PAA in both vascular and non-vascular plants, we conclude that plants generally produce two types of auxins with distinct transport characteristics.

Similar to IAA, PAA may also be produced mainly in the tip regions in maize coleoptiles since the orthologs of the *TAA* and *YUC* genes in maize, *VT2* and *SPI1*, are highly expressed in these tissues (**Fig. 5D**). It is known that IAA is basipetally transported and forms a concentration gradient from the tip downward in maize coleoptiles (Nishimura et al. 2009). Importantly, PAA also forms concentration gradients similar to IAA (**Fig. 5B, C**), although it is not actively and directionally transported in plant tissues (**Fig. 5F, G**). These results suggest that the PAA concentration gradient observed in maize coleoptiles is at least primarily established by local auxin biosynthesis and not by polar transport. To understand further the molecular mechanism of auxin gradient formation, it is important to investigate the localization of auxin biosynthesis and inactivation enzymes as well as the metabolic fate of auxins.

The exact mechanism of PAA transport in plants remains unknown. It has been demonstrated that PINs, AUX1/LAXs and ABCB transporters actively transport IAA (Friml 2010). Similarly, PINs and ABCB transporters probably play a role in the transport of NAA (Friml 2010). In contrast, AUX1 does not appear to contribute to the uptake of NAA by cells, as the root growth defects of *aux1-7* mutants are recovered by applying NAA (Yamamoto and Yamamoto 1998). Previous studies have shown that AUX1 mediates the uptake of 2,4-D into cells and that ABCB4 probably plays a role in the transmembrane movement of 2,4-D (Yang et al. 2006, Kubeš et al. 2012). Interestingly, PIN7 stimulates the efflux of 2,4-D from cells when overexpressed in BY-2 cells (Petrasek et al. 2006), even though 2,4-D is not actively and directionally transported in plant tissues. Based on these results and similar transport characteristics between PAA and 2,4-D in Arabidopsis (**Fig. 6F**), we cannot exclude the possibility that some PIN members may play a minor role in the transport of PAA. Biochemical analysis of PINs, AUX1/LAXs and ABCB transporters would help to improve our understanding of the mechanism of PAA transport in plants.

Physiological roles of PAA in plants

We showed a wide distribution of PAA in the plant kingdom and variation in PAA concentrations in Arabidopsis tissues (**Fig. 1**). These facts may imply that PAA also plays an important role as an auxin in many aspects of plant growth and development. Consistent with a previous report (Shimizu-Mitao and Kakimoto 2014), PAA promotes the interaction of TIR1/AFBs with Aux/IAAs in yeast, although the affinity of PAA for auxin co-receptors might be lower than that of IAA (**Fig. 3**). In addition, IAA and PAA up-regulate the same early auxin-responsive genes, including *Aux/IAA* and *GH3* (**Table 1**; **Supplementary Table S1**). Further analysis of the PAA-dependent interaction of TIR1/AFBs and Aux/IAAs may be important for understanding the specific role of PAA in auxin-mediated regulation.

Materials and Methods

Plant materials and growth conditions

The *Arabidopsis thaliana* ecotype Col-0 was used as the WT plant. Arabidopsis seeds were stratified at 4°C for 2 d in the dark. Seedlings were grown vertically on Murashige and Skoog (MS) medium with 1% sucrose under continuous light conditions at 20–22°C. Oats and barley were grown in soil at 20°C during the day and 15°C at night, with a 16 h photoperiod. For the analysis of auxins in vascular and non-vascular plants, 2-week-old seedlings of Arabidopsis, 7-day-old shoots of oats, 7-day-old shoots of barley, 3-week-old plants of *P. patens* and 2-week-old plants of *M. polymorpha* were used. For the analysis of auxins in Arabidopsis tissues, 3-month-old dry seeds, siliques (7 d after flowering), inflorescences, cauline leaves, stems (2 cm from the bottom end) and rosette leaves of 5-week-old plants grown in soil, and roots of 7-day-old seedlings grown on MS agar media were used. For lateral root formation analysis, WT seedlings were germinated and grown vertically on MS agar medium for 5 d and then on auxin-containing medium for 4 d ($n = 10$). The moss *P. patens* was maintained as protonemata on a plate containing BCDATG medium (Nishiyama et al. 2000). To observe their auxin response, gametophores were cultured on a plate with BCD medium (Nishiyama et al. 2000) containing 0.1 mM $CaCl_2$ and 0.1% gellan gum for 7 d. The gametophores were incubated for 7 d with 5 μM 2,4-D or PAA. For analysis of auxins in maize coleoptiles, seeds of maize (*Zea mays* L. cv. Honey Bantam 610, Sakata Seed Corp.) were germinated at 24°C under red light for 2 d and grown in darkness

for 1–2 d. Coleoptile segments (20 mm long) were prepared as previously reported (Nishimura et al. 2009) and used for NPA-dependent transport inhibition (1 h) and gravitropic stimulation (1 h) tests. A solution of 2.5 μl of NPA (200 μM NPA) was placed in the tip region inside each coleoptile. The expression levels of *VT2* and *SPI1* genes in maize coleoptiles were semi-quantitatively measured as previously described (Gallavotti et al. 2008, Phillips et al. 2011). For the *yucQ* recovery test, *yucQ* seedlings were grown in the first gravity direction (1st g) on vertical MS agar medium with auxins for 4 ds and then rotated by 90° (2nd g) and cultured for an additional 24 h. We used *pER8* and *pMDC7::YUC6* plants (Mashiguchi et al. 2011). Gateway cloning was used to construct *pMDC7::YUC1* and *pMDC7::YUC2*. The *YUC1* and *YUC2* cDNA clones were obtained from the Arabidopsis Biological Resource Center (ABRC). The coding sequences were amplified by PCR of the cDNA for *YUC1* or *YUC2* using the primers shown in **Supplementary Table S2**. The PCR products were subcloned into the entry vector pENTR/D-TOPO (Invitrogen, http://www.invitrogen.com) and shuttled into the estrogen-inducible vector pMDC7 by an LR clonase reaction (Invitrogen). The PCR was performed using the high fidelity Pyrobest DNA polymerase (TAKARA). The resulting constructs were transformed into Col-0 plants by floral dipping in *Agrobacterium tumefaciens* liquid cultures. For β-estradiol treatment, seedlings were grown vertically on MS agar media for 7 d and then transferred to MS agar media containing 10 μM β-estradiol and grown for another 3 d. For the analysis of *YUC* gene expression levels, total RNA was isolated from plants using the RNeasy Plant Mini Kit (Qiagen). A 1 μg aliquot of total RNA was used for cDNA synthesis using a QuantiTect Reverse Transcription kit (Qiagen). Quantitative RT–PCR was performed on a 7500 Real-time PCR system (Applied Biosystems) using a THUNDERBIRD SYBR qPCR mix (Toyobo) and the specific primers listed in **Supplementary Table S2**. 18S rRNA expression was used as an internal standard. For the analysis of auxins in the inflorescence parts of 5-week-old *yuc1 yuc2 yuc6*, we identified triple knockout mutants from the progeny of *yuc1 yuc2/+ yuc4/+ yuc6* plants by genotyping. The *GH3.9* gene was reported as a causal gene of a dominant mutant (Khan and Stone 2007). We also identified a new allele of *GH3.9* as a dwarf dominant mutant through an activation tagging method. To construct *pER8::GH3.9*, the genomic sequence was amplified using the primers shown in **Supplementary Table S2**. The amplified fragment was cloned into vector pER8. The resulting construct, *pER8::GH3.9*, was transformed into Arabidopsis *DR5::GFP* using floral dipping in *A. tumefaciens* liquid culture.

Chemicals and general experimental conditions

All chemicals were purchased from Sigma-Aldrich unless otherwise stated. All ^{13}C-labeled chemicals were purchased from Cambridge Isotope Laboratories. PAA was obtained from Wako Pure Chemical Industries. Mass spectra were measured using a Q-Tof-premier instrument (Waters) or Agilent 6410 Triple Quad system (Agilent).

Analysis of auxins and their metabolites

LC-ESI-MS/MS analysis of IAA and IAA–amino acid conjugates was performed as previously described (Mashiguchi et al. 2011). The analysis of PAA was performed with the same procedure as for IAA. As an internal standard, [phenyl-$^{13}C_6$]PAA was added before the homogenization of plant tissues in 80% acetone/H_2O. In HPLC, fractions eluting at 7–9 min were collected, combined, and evaporated using a Speed Vac (Thermo) at 35°C. The dried PAA fraction was further purified using an Oasis HLB column (1 ml, Waters) with the same procedure as for IAA, and then evaporated to dryness using a Speed Vac. The fraction was redissolved in 1% acetic acid/H_2O (10–20 μl) and injected into an ACQUITY ultra performance liquid chromatography (UPLC)-MS/MS Q-Tof-premier system (Waters). UPLC was carried out with 0.05% acetic acid (solvent A2) and acetonitrile with 0.05% acetic acid (solvent B2) using 2% solvent B2 for 0.2 min and a gradient from 2% to 50% of solvent B2 for 7.3 min at a flow rate of 0.2 ml min^{-1}. The temperature of the UPLC column was set to 40°C. The MS/MS analysis conditions for PAA and [phenyl-$^{13}C_6$]PAA (negative ion mode) were as follows: capillary = 2.65 kV, source temperature = 100°C, desolvation temperature = 400°C, collision energy = 1.5 eV, sampling cone voltage = 10 V, scan time = 0.6 s scan^{-1} (delay = 0.05 s) and MS/MS transition (*m*/z) = 135.1/91.1 for unlabeled PAA and 141.1/97.1 for [phenyl-$^{13}C_6$]PAA.

PAA–amino acid conjugates were purified with IAA–amino acid conjugates using a previously reported method (Mashiguchi et al. 2011). As internal standards, [$^{13}C_4$, ^{15}N]PAA-Asp and [$^{13}C_5$, ^{15}N]PAA-Glu were added before homogenization. In HPLC, we collected and combined the fractions eluting at 3–7 min in which both IAA– and PAA–amino acid conjugates were eluted. After evaporation using a Speed Vac, the dried IAA– and PAA–amino acid conjugate fraction was redissolved with 1% acetic acid/H_2O and purified using an Oasis MCX column (1 ml) and an Oasis MAX column (1 ml, Waters), and then the eluate was evaporated to dryness. The fraction was redissolved in 1% acetic acid/H_2O (10–20 μl) and analyzed independently by the UPLC-ESI-MS/MS system. UPLC for all amino acid conjugates was carried out with solvent A2 and solvent B2 using 10% solvent B2 for 1 min and a gradient from 10% to 50% solvent B2 for 6 min at a flow rate of 0.2 ml min^{-1}. The temperature of the UPLC column was set to 30°C. The retention time of PAA-Asp/[$^{13}C_4$, ^{15}N]PAA-Asp was 2.81 min and that of PAA-Glu/[$^{13}C_5$, ^{15}N]PAA-Glu was 3.17 min. The MS/MS analysis conditions (negative ion mode) for PAA-Asp/[$^{13}C_4$, ^{15}N]PAA-Asp were as follows: capillary = 2.65 kV, source temperature = 100°C, desolvation temperature = 400°C, collision energy = 8 eV, sampling cone voltage = 20 V, scan time 0.6 s scan^{-1} (delay = 0.05 s) and MS/MS transition (*m*/z) = 250.1/132.1 for unlabeled PAA-Asp and 255.1/137.1 for [$^{13}C_4$, ^{15}N]PAA-Asp. The MS/MS analysis conditions for PAA-Glu and [$^{13}C_5$, ^{15}N] PAA-Glu were as follows: capillary = 2.65 kV, source temperature = 100°C, desolvation temperature = 400°C, collision energy = 8 eV, sampling cone voltage = 19 V, scan time = 0.6 s scan^{-1} (delay = 0.05 s) and MS/MS transition (*m*/z) = 264.1/146.1 for unlabeled PAA-Glu and 270.1/152.1 for [$^{13}C_5$, ^{15}N]PAA-Glu. Quantification was carried out using the extracted ion chromatogram of PAA-Asp and [$^{13}C_4$, ^{15}N]PAA-Asp or PAA-Glu and [$^{13}C_5$, ^{15}N]PAA-Glu. Standard curves were generated using the ratios between labeled standards and unlabeled compounds in the mixture. UPLC-MS/MS analysis conditions and quantification for IAA amino acid conjugates were the same as previously reported (Mashiguchi et al. 2011).

Alternatively, we used an Agilent 6410 Triple Quad system (Agilent) for LC-ESI-MS/MS analysis of IAA and PAA. Frozen plant tissues (30–150 mg) were homogenized with zirconia beads (3 mm) in 0.3–1.5 ml of 80% acetonitrile/1% acetic acid/H_2O containing [phenyl-$^{13}C_6$]IAA and [phenyl-$^{13}C_6$]PAA by using a Tissue Lyser (Qiagen) for 3 min. Extracts were centrifuged at 13,000 × *g* for 3 min under 4°C, and the supernatant was collected. Extraction was repeated once without [phenyl-$^{13}C_6$]IAA and [phenyl-$^{13}C_6$]PAA. Extracts were combined and the volume was reduced to $<$100 μl by evaporation using a Speed Vac. Then, extracts were loaded onto an Oasis HLB column (1 ml, Waters), and washed with 1% acetic acid/H_2O (1 ml). IAA and PAA were eluted with 80% acetonitrile/1% acetic acid/H_2O (2 ml), and the fraction was reduced to $<$100 μl. The fraction containing both IAA and PAA was loaded onto an Oasis WAX column (1 ml). After washing with 1% acetic acid/H_2O (1 ml) and 80% acetonitrile/H_2O (2 ml), IAA and PAA were eluted with 80% acetonitrile/1% acetic acid/H_2O (2 ml) and evaporated. The fraction was redissolved in 1% acetic acid/H_2O (30 μl) and injected into an Agilent 6410 Triple Quad system with a ZORBAX Eclipse XDB-C18 column (1.8 μm, 2.1 × 50 mm). HPLC was carried out with 0.01% acetic acid/H_2O (solvent A) and acetonitrile/0.05% acetic acid (solvent B) using 3% solvent B for 3 min and a gradient from 3% to 15% of solvent B over 20 min at a flow rate of 0.2 ml min^{-1}. The temperature of the UPLC column was set to 40°C. The MS/MS analysis conditions for IAA and [phenyl-$^{13}C_6$]IAA (positive ion mode) were as follows: capillary = 4,000 V, fragmentor voltage = 120 V, collision energy = 18 V, dwell time = 500 ms and MS/MS transition (*m*/z) = 176/130 for unlabeled IAA and 182/136 for [phenyl-$^{13}C_6$]IAA. The MS/MS analysis conditions for PAA and [phenyl-$^{13}C_6$]PAA (negative ion mode) were as follows: capillary = 4,000 V, fragmentor voltage = 55 V, collision energy = 1 V, dwell time = 500 ms and MS/MS transition (*m*/z) = 135/91 for unlabeled PAA and 141/97 for [phenyl-$^{13}C_6$]PAA.

Enzyme assay of YUC2

The GST-fused YUC2 protein (GST–YUC2) was expressed in *E. coli* and purified as previously described (Mashiguchi et al. 2011). GST–YUC2 activity was assayed at 30°C for 20 min in 100 μl of a reaction buffer containing 20 μg of GST–YUC2, 50 μM IPA or PPA, 40 μM FAD and 1 mM NADPH in PBS buffer (pH 7.4). IPA or PPA was added to the reaction just before incubation at 30°C.

For a control, the assay was performed without NADPH. Enzyme reactions were stopped by the addition of 100 µl acetonitrile, and then 4 µl (IPA) or 1.2 µl (PPA) of the mixtures was analyzed by UPLC-ESI-MS/MS using the negative ion mode. UPLC was carried out with solvent A2 and solvent B2 using 2% solvent B2 for 1.0 min and a gradient from 2% to 80% solvent B2 for 7.5 min at a flow rate of 0.2 ml min^{-1}. The temperature of the UPLC column was 30°C. MS/MS analysis conditions for IAA, PPA and PAA were as follows: capillary = 2.65 kV; source temperature = 100°C; desolvation temperature = 400°C; collision energy = 7 eV for IAA and PPA and 2.0 eV for PAA; sampling cone voltage = 10 V; and MS/MS transition (*m/z*) = 174.1/130.1 for IAA, 163.1/91.1 for PPA and 135.1/91.1 for PAA. IPA was monitored by its precursor ion (*m/z* 202.1) with conditions as follows: capillary = 2.65 kV; source temperature = 100°C; desolvation temperature = 400°C; collision energy = 0.2 eV; and sampling cone voltage = 10 V. The identities of these compounds were also confirmed by the retention times of authentic compounds.

Microarray analysis

Seedlings of Col-0 were germinated and grown on MS agar medium for 1 week, then transferred to MS liquid medium (15 ml) and cultured with rotation (200 r.p.m.) for 1 week. Then, seedlings were cultured with 1 µM IAA or 10 µM PAA or mock solution in MS liquid medium for 1 h with three replications. Total RNA was isolated using RNeasy (Qiagen). cRNA amplification and fluorescence labeling were performed using the Agilent Low RNA Input Linear Amplification Kit (Agilent Technology). A primer containing poly(dT) and a T7 polymerase promoter was annealed to the poly(A)$^+$ RNA. First- and second-strand cDNA were reverse transcribed from 500 ng of total RNA using an MMLV-RT enzyme. Cyanine 3-labeled cRNA was synthesized using T7 RNA polymerase. Labeled cRNA was purified by an RNeasy Mini Kit (Qiagen). Hybridization was performed using the GeneChip Eukaryotic Hybridization Control Kit (Affymetrix) on an ATH1 GeneChip array (Affymetrix). The hybridized and washed material on each glass slide was scanned by a Fluidics Station 400 (Affymetrix). Data analysis was performed using Microarray Suite (Affymetrix). The array intensities were processed using the Bioconductor (www.bioconductor.org) affy package in the R software environment (www.r-project.org). Hybridization intensities among arrays were normalized by quantile normalization. The degree of differential regulation was inferred by the R library 'Limma.' The FDR was calculated by the Limma application (Smyth et al. 2005). Correlation analysis was performed using the cor.test function in the R software environment.

DR5::GUS reporter assay

A 5-day-old *Arabidopsis DR5::GUS* reporter line was incubated for 5 h in half-strength MS liquid medium containing chemicals and auxins under continuous white light at 24°C. For histochemical GUS enzyme staining, the *DR5::GUS* reporter seedlings were washed with a GUS staining buffer [100 mM sodium phosphate, pH 7.0, 10 mM EDTA, 0.5 mM $K_4Fe(CN)_6$, 0.5 mM $K_3Fe(CN)_6$ and 0.1% Triton X-100] after hormonal induction and transferred to a GUS staining buffer containing 1 mM 5-bromo-4-chloro-3-indolyl-β-D-glucuronide. The seedlings were then incubated at 37°C until sufficient staining developed.

Yeast two-hybrid assay and pull-down assay

A yeast two-hybrid assay and pull down assay were performed twice as previously published (Calderon Villalobos et al. 2012, Yu et al. 2013).

Supplementary data

Supplementary data are available at PCP online.

Funding

This study was supported by the Japan Society for the Promotion of Science (JSPS) [KAKENHI Grants 22780108 (to K.M.), 25114518 (to K.-i.H.) and 24370027 (to H.K)]; National Instiutes of Health (NIH) [grants GM43644 (to M.E.) and GM114660 (to Y.Z.)]; the Howard Hughes Medical Insitute (HHMI) and the Gordon and Betty Moore Foundation (GBMF) [to M.E.]; the Ministry of Education, Culture, Sports, Science and Technology (MEXT) [a MEXT matching fund subsidy for private universities for 2009–2013 (to K.-i.H.)]; Japan Science and Technology Agency (JST) [PRESTO (to H.K.)].

Acknowledgments

We thank Dr. Belay T. Ayele and Dr. Hitoshi Sakakibara for comments on the manuscript, and Ms. Aya Ide for assistance in preparing the plant materials. Yeast strains were provided by the National Bio-Resource Project (NBRP) of the Ministry of Education, Culture, Sports, Science, and Technology (MEXT), Japan.

Disclosures

The authors have no conflicts of interest to declare.

References

Bak, S., Nielsen, H.L. and Halkier, B.A. (1998) The presence of CYP79 homologues in glucosinolate-producing plants shows evolutionary conservation of the enzymes in the conversion of amino acid to aldoxime in the biosynthesis of cyanogenic glucosides and glucosinolates. *Plant Mol. Biol.* 38: 725–734.

Barbez, E., Kubeš, M., Rolcik, J., Béziat, C., Pěnčík, A., Wang, B., et al. (2012) A novel putative auxin carrier family regulates intracellular auxin homeostasis in plants. *Nature* 485: 119–122.

Beyer, E.M. (1972) Auxin transport: a new synthetic inhibitor. *Plant Physiol.* 50: 322–327.

Brumos, J., Alonso, J.M. and Stepanova, A.N. (2014) Genetic aspects of auxin biosynthesis and its regulation. *Physiol. Plant.* 151: 3–12.

Calderon Villalobos, L.I., Lee, S., De Oliveira, C., Ivetac, A., Brandt, W., Armitage, L., et al. (2012) A combinatorial TIR1/AFB–Aux/IAA co-receptor system for differential sensing of auxin. *Nat. Chem. Biol.* 8: 477–485.

Calderon-Villalobos, L.I., Tan, X., Zheng, N. and Estelle, M. (2010) Auxin perception—structural insights. *Cold Spring Harb. Perspect. Biol.* 2: a005546.

Chen, Q., Dai, X., De-Paoli, H., Cheng, Y., Takebayashi, Y., Kasahara, H., et al. (2014) Auxin overproduction in shoots cannot rescue auxin deficiencies in Arabidopsis roots. *Plant Cell Physiol.* 55: 1072–1079.

Cheng, Y., Dai, X. and Zhao, Y. (2006) Auxin biosynthesis by the YUCCA flavin monooxygenases controls the formation of floral organs and vascular tissues in *Arabidopsis*. *Genes Dev.* 20: 1790–1799.

Dai, X., Mashiguchi, K., Chen, Q., Kasahara, H., Kamiya, Y., Ojha, S., et al. (2013) The biochemical mechanism of auxin biosynthesis by an *Arabidopsis* YUCCA flavin-containing monooxygenase. *J. Biol. Chem.* 288: 1448–1457.

Davies, P.J. (2004) The plant hormones: their nature, occurrence, and functions. *In* Plant Hormones—Biosynthesis, Signal Transduction, Action! Edited by Davies, P.J. pp. 1–15. Kluwer Academic Publishers, Dordrecht.

Delbarre, A., Muller, P., Imhoff, V. and Guern, J. (1996) Comparison of mechanisms controlling uptake and accumulation of

2,4-dichlorophenoxy acetic acid, naphthalene-1-acetic acid, and indole-3-acetic acid in suspension-cultured tobacco cells. *Planta* 198: 532–541.

Dharmasiri, N., Dharmasiri, S. and Estelle, M. (2005) The F-box protein TIR1 is an auxin receptor. *Nature* 435: 441–445.

Friml, J. (2010) Subcellular trafficking of PIN auxin efflux carriers in auxin transport. *Eur. J. Cell Biol.* 89: 231–235.

Gallavotti, A., Barazesh, S., Malcomber, S., Hall, D., Jackson, D., Schmidt, R.J., et al. (2008) *sparse inflorescence1* encodes a monocot-specific *YUCCA*-like gene required for vegetative and reproductive development in maize. *Proc. Natl Acad. Sci. USA* 105: 15196–15201.

Goda, H., Sawa, S., Asami, T., Fujioka, S., Shimada, Y. and Yoshida, S. (2004) Comprehensive comparison of auxin-regulated and brassinosteroid-regulated genes in Arabidopsis. *Plant Physiol.* 134: 1555–1573.

Haagen Smit, A.J. and Went, F.W. (1935) A physiological analysis of the growth substance. *Proc. R. Acad. Amsterdam* 38: 852–857.

Hayashi, K., Neve, J., Hirose, M., Kuboki, A., Shimada, Y., Kepinski, S., et al. (2012) Rational design of an auxin antagonist of the SCF(TIR1) auxin receptor complex. *ACS Chem. Biol.* 7: 590–598.

Hayashi, K., Tan, X., Zheng, N., Hatate, T., Kimura, Y., Kepinski, S., et al. (2008) Small-molecule agonists and antagonists of F-box protein–substrate interactions in auxin perception and signaling. *Proc. Natl Acad Sci. USA* 105: 5632–5637.

Hull, A.K., Vij, R. and Celenza, J.L. (2000) *Arabidopsis* cytochrome P450s that catalyze the first step of tryptophan-dependent indole-3-acetic acid biosynthesis. *Proc. Natl Acad. Sci. USA* 97: 2379–2384.

Jackson, R.G., Kowalczyk, M., Li, Y., Higgins, G., Ross, J., Sandberg, G., et al. (2002) Over-expression of an *Arabidopsis* gene encoding a glucosyltransferase of indole-3-acetic acid: phenotypic characterisation of transgenic lines. *Plant J.* 32: 573–583.

Jacobs, W.P., McCready, C.C. and Osborne, D.J. (1966) Transport of the auxin 2,4-dichlorophenoxyacetic acid through absiccion zones, pulvini, and petioles of Phaseolus vulgaris. *Plant Physiol.* 41: 725–730.

Kepinski, S. and Leyser, O. (2005) The Arabidopsis F-box protein TIR1 is an auxin receptor. *Nature* 435: 446–451.

Khan, S. and Stone, J.M. (2007) *Arabidopsis thaliana* GH3.9 influences primary root growth. *Planta* 226: 21–34.

Korasick, D.A., Enders, T.A. and Strader, L.C. (2013) Auxin biosynthesis and storage forms. *J. Exp. Bot.* 64: 2541–2555.

Kubeš, M., Yang, H., Richter, G.L., Cheng, Y., Mł odzińska, E., Wang, X., et al. (2012) The Arabidopsis concentration-dependent influx/efflux transporter ABCB4 regulates cellular auxin levels in the root epidermis. *Plant J.* 69: 640–654.

Ljung, K., Bhalerao, R.P. and Sandberg, G. (2001) Sites and homeostatic control of auxin biosynthesis in *Arabidopsis* during vegetative growth. *Plant J.* 28: 465–474.

Löbler, M. and Klämbt, D. (1985) Auxin-binding protein from coleoptile membranes of corn (*Zea mays* L.). I. Purification by immunological methods and characterization. *J. Biol. Chem.* 260: 9848–9853.

Ludwig-Müller, J. and Cohen, J.D. (2002) Identification and quantification of three active auxins in different tissues of *Tropaeolum majus*. *Physiol. Plant.* 115: 320–329.

Mashiguchi, K., Tanaka, K., Sakai, T., Sugawara, S., Kawaide, H., Natsume, M., et al. (2011) The main auxin biosynthesis pathway in *Arabidopsis*. *Proc. Natl Acad. Sci. USA* 108: 18512–18517.

Mikkelsen, M.D., Hansen, C.H., Wittstock, U. and Halkier, B.A. (2000) Cytochrome P450 CYP79B2 from *Arabidopsis* catalyzes the conversion of tryptophan to indole-3-acetaldoxime, a precursor of indole glucosinolates and indole-3-acetic acid. *J. Biol. Chem.* 275: 33712–33717.

Morris, D.A. and Johnson, C.F. (1987) Regulation of auxin transport in pea (*Pisum sativum* L.) by phenylacetic acid: inhibition of polar auxin transport in intact plants and stem segments. *Planta* 172: 408–416.

Muir, R.M., Fujita, T. and Hansch, C. (1967) Structure–activity relationship in the auxin activity of mono-substituted phenylacetic acids. *Plant Physiol.* 42: 1519–1526.

Nemhauser, J.L., Hong, F. and Chory, J. (2006) Different plant hormones regulate similar processes through largely nonoverlapping transcriptional responses. *Cell* 126: 467–475.

Nishimura, T., Nakano, H., Hayashi, K., Niwa, C. and Koshiba, T. (2009) Differential downward stream of auxin synthesized at the tip has a key role in gravitropic curvature via TIR1/AFBs-mediated auxin signaling pathways. *Plant Cell Physiol.* 50: 1874–1885.

Nishiyama, T., Hiwatashi, Y., Sakakibara, I., Kato, M. and Hasebe, M. (2000) Tagged mutagenesis and gene-trap in the moss, *Physcomitrella patens* by shuttle mutagenesis. *DNA Res.* 7: 9–17.

Parry, G., Calderon-Villalobos, L.I., Prigge, M., Peret, B., Dharmasiri, S., Itoh, H., et al. (2009) Complex regulation of the TIR1/AFB family of auxin receptors. *Proc. Natl Acad. Sci. USA* 106: 22540–22545.

Pěnčík, A., Simonovik, B., Petersson, S.V., Henyková, E., Simon, S., Greenham, K., et al. (2013) Regulation of auxin homeostasis and gradients in *Arabidopsis* roots through the formation of the indole-3-acetic acid catabolite 2-oxindole-3-acetic acid. *Plant Cell* 25: 3858–3870.

Petrasek, J., Mravec, J., Bouchard, R., Blakeslee, J.J., Abas, M., Seifertova, D., et al. (2006) PIN proteins perform a rate-limiting function in cellular auxin efflux. *Science* 312: 914–918.

Phillips, K.A., Skirpan, A.L., Liu, X., Christensen, A., Slewinski, T.L., Hudson, C., et al. (2011) *vanishing tassel2* encodes a grass-specific tryptophan aminotransferase required for vegetative and reproductive development in maize. *Plant Cell* 23: 550–566.

Procházka, S. and Borkovec, V. (1984) Transport and regulative properties of phenylacetic acid. *Biol. Plant.* 26: 358–363.

Qin, G., Gu, H., Zhao, Y., Ma, Z., Shi, G., Yang, Y., et al. (2005) An indole-3-acetic acid carboxyl methyltransferase regulates *Arabidopsis* leaf development. *Plant Cell* 17: 2693–2704.

Schneider, E.A., Kazakoff, C.W. and Wightman, F. (1985) Gas chromatography–mass spectrometry evidence for several endogenous auxins in pea seedling organs. *Planta* 165: 232–241.

Shimizu-Mitao, Y. and Kakimoto, T. (2014) Auxin sensitivities of all Arabidopsis Aux/IAAs for degradation in the presence of every TIR1/AFB. *Plant Cell Physiol.* 55: 1450–1459.

Simon, S. and Petrasek, J. (2011) Why plants need more than one type of auxin. *Plant Sci.* 180: 454–460.

Small, D.K. and Morris, D.A. (1990) Promotion of elongation and acid invertase activity in *Phaseolus vulgaris* L. internode segments by phenylacetic acid. *Plant Growth Regul.* 9: 329–340.

Smyth, G.K., Michaud, J. and Scott, H.S. (2005) Use of within-array replicate spots for assessing differential expression in microarray experiments. *Bioinformatics* 21: 2067–2075.

Staswick, P.E., Serban, B., Rowe, M., Tiryaki, I., Maldonado, M.T., Maldonado, M.C., et al. (2005) Characterization of an Arabidopsis enzyme family that conjugates amino acids to indole-3-acetic acid. *Plant Cell* 17: 616–627.

Stepanova, A.N., Robertson-Hoyt, J., Yun, J., Benavente, L.M., Xie, D.Y., Doležal, K., et al. (2008) *TAA1*-mediated auxin biosynthesis is essential for hormone crosstalk and plant development. *Cell* 133: 177–191.

Stepanova, A.N., Yun, J., Robles, L.M., Novak, O., He, W., Guo, H., et al. (2011) The *Arabidopsis* YUCCA1 flavin monooxygenase functions in the indole-3-pyruvic acid branch of auxin biosynthesis. *Plant Cell* 23: 3961–3973.

Sugawara, S., Hishiyama, S., Jikumaru, Y., Hanada, A., Nishimura, T., Koshiba, T., et al. (2009) Biochemical analyses of indole-3-acetaldoxime-dependent auxin biosynthesis in *Arabidopsis*. *Proc. Natl Acad. Sci. USA* 106: 5430–5435.

Suttle, J.C. and Mansager, E.R. (1986) The physiological significance of phenylacetic acid in abscising cotton cotyledons. *Plant Physiol.* 81: 434–438.

Swarup, R. and Peret, B. (2012) AUX/LAX family of auxin influx carriers—an overview. *Front. Plant Sci.* 3: 225.

Tanaka, K., Hayashi, K., Natsume, M., Kamiya, Y., Sakakibara, H., Kawaide, H., et al. (2014) UGT74D1 catalyzes the glucosylation of 2-oxindole-3-acetic acid in the auxin metabolic pathway in *Arabidopsis*. *Plant Cell Physiol.* 55: 218–228.

Tao, Y., Ferrer, J.L., Ljung, K., Pojer, F., Hong, F., Long, J.A., et al. (2008) Rapid synthesis of auxin via a new tryptophan-dependent pathway is required for shade avoidance in plants. *Cell* 133: 164–176.

Van Overbeek, J. (1959) Auxins. *Bot. Rev.* 25: 269–350.

Wightman, F. and Lighty, D.L. (1982) Identification of phenylacetic acid as natural auxin in the shoots of higher plants. *Physiol. Plant.* 55: 17–24.

Wittstock, U. and Halkier, B.A. (2000) Cytochrome P450 CYP79A2 from *Arabidopsis thaliana* L. catalyzes the conversion of l-phenylalanine to phenylacetaldoxime in the biosynthesis of benzylglucosinolate. *J. Biol. Chem.* 275: 14659–14666.

Won, C., Shen, X., Mashiguchi, K., Zheng, Z., Dai, X., Cheng, Y., et al. (2011) Conversion of tryptophan to indole-3-acetic acid by TRYPTOPHAN AMINOTRANSFERASES OF *ARABIDOPSIS* and YUCCAs in *Arabidopsis*. *Proc. Natl Acad. Sci. USA* 108: 18518–18523.

Yamamoto, M. and Yamamoto, K.T. (1998) Differential effects of 1-naphthaleneacetic acid, indole-3-acetic acid and 2,4-dichlorophenoxyacetic acid on the gravitropic response of roots in an auxin-resistant mutant of arabidopsis, *aux1*. *Plant Cell Physiol.* 39: 660–664.

Yang, Y., Hammes, U.Z., Taylor, C.G., Schachtman, D.P. and Nielsen, E. (2006) High-affinity auxin transport by the AUX1 influx carrier protein. *Curr. Biol.* 16: 1123–1127.

Yu, H., Moss, B.L., Jang, S.S., Prigge, M., Klavins, E., Nemhauser, J.L., et al. (2013) Mutations in the TIR1 auxin receptor that increase affinity for auxin/indole-3-acetic acid proteins result in auxin hypersensitivity. *Plant Physiol.* 162: 295–303.

Zhao, Y. (2012) Auxin biosynthesis: a simple two-step pathway converts tryptophan to indole-3-acetic acid in plants. *Mol. Plant* 5: 334–338.

Zhao, Y., Christensen, S.K., Fankhauser, C., Cashman, J.R., Cohen, J.D., Weigel, D., et al. (2001) A role for flavin monooxygenase-like enzymes in auxin biosynthesis. *Science* 291: 306–309.

Zhao, Z., Zhang, Y., Liu, X., Zhang, X., Liu, S., Yu, X., et al. (2013) A role for a dioxygenase in auxin metabolism and reproductive development in rice. *Dev Cell* 27: 113–122.